Journal of Molecular Science

Journal of Molecular Science
Volume 35 Issue 4, Year of Publication 2025, Page 1779-1785
DoI-10.004687/1000-9035.2025.240

Journal of Molecular Science
www.jmolecularsci.com ISSN:1000-9035

In Silico ADMET Profiling of Novel Pyrimidine Derivatives as Potential Kinase Inhibitors

Bharti Patel *[1], Akash Luniya[1], Anurag Dohare[1], Ansari Rehan Mohd Muqeem[1], Mohammad Wasim[1], Mohd Asim Jamil Ahmad[1], Ansari Shehbaz Mohd Shoeb[2]

[1]SAM College of Pharmacy, Faculty of Medical and Paramedical Sciences, SAM Global University Raisen-(MadhyaPradesh) India- 464551

[2]School of Pharmacy, Faculty of Medical and Paramedical Sciences, SAM Global University Raisen-(MadhyaPradesh) India- 464551

Article Information
Received: 06-08-2025
Revised: 28-09-2025
Accepted: 12-11-2025
Published: 24-12-2025

Keywords
ADMET profiling; kinase inhibitors; pyrimidine derivatives; SwissADME; drug-likeness; in silico toxicology

ABSTRACT

Kinase inhibitors represent one of the most successful classes of targeted anticancer agents. In this study, eight novel pyrimidine derivatives (PY-01 to PY-08) were designed and subjected to comprehensive in silico ADMET (Absorption, Distribution, Metabolism, Excretion and Toxicity) profiling using SwissADME, pkCSM and ADMETlab 2.0 platforms. Physicochemical analysis demonstrated that all derivatives complied with Lipinski's Rule of Five (MW: 298–387 Da; LogP: 1.98–3.87; HBD: 1–3; HBA: 5–7). The BOILED-Egg model confirmed favourable gastrointestinal absorption for all compounds. PY-04 and PY-06 emerged as lead candidates, displaying high human intestinal absorption (94.6% and 96.2%, respectively), superior Caco-2 permeability, low hERG cardiotoxicity probability, and negative AMES mutagenicity. Metabolic stability assessments indicated minimal CYP450 interactions for PY-04 and PY-06. These findings strongly support the further development of PY-04 and PY-06 as promising pyrimidine-based kinase inhibitor candidates warranting in vitro and in vivo validation.

INTRODUCTION:

Protein kinases regulate virtually every facet of cellular signalling, governing proliferation, differentiation, survival, and motility. With over 500 human kinase genes constituting approximately 2% of the genome, dysregulated kinase activity is implicated in the pathogenesis of cancer, inflammatory disorders, and metabolic diseases.[1,2] The approval of imatinib mesylate in 2001 as the first targeted kinase inhibitor transformed oncology practice and validated kinase inhibition as a clinically actionable therapeutic strategy.3 Subsequent decades have witnessed the regulatory approval of more than 70 small-molecule kinase inhibitors spanning diverse target classes, including BCR-ABL, EGFR, VEGFR, CDK, and PI3K, underscoring the robustness of this target class.[4,5]

The pyrimidine scaffold is a privileged pharmacophore in medicinal chemistry, appearing in numerous FDA-approved kinase inhibitors such as imatinib, dasatinib, gefitinib, and erlotinib.[6,7] The bicyclic or substituted monocyclic pyrimidine ring confers the structural flexibility necessary for establishing key hydrogen bond interactions within the ATP-binding cleft of kinases, particularly with the hinge region residues.8 The introduction of diverse substituents at the 2-, 4-, and 5-positions of the pyrimidine core has been widely exploited to modulate selectivity, potency, and pharmacokinetic profiles.[9,10]

Despite the prolific output of synthetic medicinal chemistry efforts, attrition due to suboptimal pharmacokinetic and toxicological profiles remains a primary cause of late-stage clinical failure.11 It has been estimated that 40–50% of drug candidates fail in development due to poor ADMET properties.[12]

Consequently, early integration of in silico ADMET screening into the drug discovery workflow has emerged as an indispensable strategy to prioritise compounds with acceptable pharmacokinetic behaviour before resource-intensive biological evaluation.[13,14]

Computational ADMET prediction tools, including SwissADME,[15] pkCSM,[16] and ADMETlab 2.0,[17] leverage quantitative structure-property relationship (QSPR) models and machine learning algorithms trained on large experimental datasets to predict key parameters such as intestinal absorption, blood-brain barrier penetration, plasma protein binding, CYP450 enzyme interactions, half-life, hERG inhibition, and AMES mutagenicity.[18,19] These tools offer rapid, cost-effective virtual screening of candidate molecules and enable rationalised structural optimisation.[20]

In this study, we report the in silico ADMET profiling of eight novel pyrimidine derivatives (PY-01 to PY-08) rationally designed to target the ATP-binding domain of kinases. Physicochemical descriptors, drug-likeness scores, and comprehensive toxicity parameters were computed and benchmarked against the approved kinase inhibitor imatinib. The objective was to identify lead candidates with optimal pharmacokinetic profiles for progression to experimental validation.

2. MATERIALS AND METHODS:

2.1 Compound Design and Structure Preparation:

Eight novel pyrimidine derivatives (PY-01 to PY-08) were designed based on the core 2-aminopyrimidine scaffold, a recurring pharmacophoric motif in clinical kinase inhibitors.21 Structural diversity was introduced by varying substituents at the 4- and 5-positions of the pyrimidine ring, incorporating sulfonamide, methoxy, and amino functional groups to modulate electronic and steric properties. Two-dimensional (2D) chemical structures were drawn using ChemDraw Professional 22.0 (PerkinElmer, USA) and exported as SMILES strings. Three-dimensional (3D) structures were generated using the CORINA online server with energy minimisation performed by the MMFF94 force field in Open Babel 3.1.1.22 Imatinib was included as a reference compound for comparative analysis.

2.2 Physicochemical Property Calculation

Physicochemical descriptors were computed using the SwissADME web server (http://www.swissadme.ch), which employs SMILES as input to calculate molecular weight (MW), partition coefficient (LogP using the iLOGP, XLOGP3, and WLOGP algorithms), topological polar surface area (TPSA), number of hydrogen bond donors (HBD) and acceptors (HBA), and number of rotatable bonds (nRotB).15 Drug-likeness was evaluated against Lipinski's Rule of Five (MW ≤ 500 Da; LogP ≤ 5; HBD ≤ 5; HBA ≤ 10),23 Veber's rule (nRotB ≤ 10; TPSA ≤ 140 Å²),24 Egan's rule (TPSA ≤ 131.6 Å²; WLOGP ≤ 5.88),25 and Muegge's rule.26 Oral bioavailability scores were assigned according to the Egan egg model implemented within SwissADME.

2.3 ADMET Profiling

Absorption parameters including human intestinal absorption (HIA), Caco-2 cell permeability, and P-glycoprotein (Pgp) substrate probability were predicted using pkCSM (https://biosig.lab.uq.edu.au/pkcsm).16 This server employs graph-based signatures trained on curated experimental datasets. Distribution parameters comprising volume of distribution (VD), blood-brain barrier (BBB) penetration, and plasma protein binding (PPB) were likewise extracted from pkCSM. Metabolic liability was assessed by predicting CYP3A4 substrate activity and CYP2D6 inhibitory potential, as these isoforms mediate the hepatic metabolism of the majority of approved drugs.27 Renal half-life (T½) and total clearance were obtained from ADMETlab 2.0.17

2.4 Toxicity Assessment

In silico toxicological profiling was performed using three complementary platforms: ProTox-II (https://tox-new.charite.de/protox_II) for acute oral toxicity (LD50) prediction,28pkCSM for hERG channel inhibition probability (cardiotoxicity), and the AMES mutagenicity predictor within ADMETlab 2.0.17hERG inhibition was classified as low (probability < 0.20), medium (0.20–0.45), or high (> 0.45) risk.29 The BOILED-Egg graphical model was generated via SwissADME, plotting TPSA versus Wlogp to visualise passive transcellular permeation and BBB partitioning for all compounds.15

2.5 Data Analysis

All predicted numerical values are reported as means from triplicate independent submissions to each server to account for any server-side stochastic variability. Data visualisation including radar plots, bar graphs, BOILED-Egg scatter plots, and toxicity profiles were generated in Python 3.11 using Matplotlib 3.8 and NumPy 1.25. Statistical comparisons between compound ADMET scores and the reference compound were conducted using one-way analysis of variance (ANOVA) with Tukey's post-hoc test ($p < 0.05$ considered significant) in GraphPad Prism 10.0.

3. RESULTS

3.1 Physicochemical Properties and Drug-

Journal of Molecular Science
Journal of Molecular Science
Volume 35 Issue 4, Year of Publication 2025, Page 1779-1785
DoI-10.004687/1000-9035.2025.240

likeness

The physicochemical descriptors of all eight pyrimidine derivatives and the reference compound are summarised in Table 1. All compounds exhibited molecular weights ranging from 298.33 Da (PY-04) to 387.44 Da (PY-07), well below the 500 Da Lipinski threshold. LogP values spanned 1.98 to 3.87, with PY-04 (1.98) demonstrating the highest hydrophilicity and PY-07 (3.87) the greatest lipophilicity within the series, all remaining below the permissible limit of 5. The number of hydrogen bond donors (HBD: 1–3) and acceptors (HBA: 5–7) were well within Lipinski's Rule of Five criteria for all compounds. Notably, PY-03 and PY-08 displayed higher HBD counts (3 each) owing to their triol-substituted amino groups. Topological polar surface area values ranged from 76.2 Å² (PY-06) to 110.4 Å² (PY-03), all below the 140 Å² threshold predictive of poor oral absorption. No compound recorded any Lipinski violations; however, PY-03 and PY-07 failed Veber's rotatable bond criterion (nRotB = 6), as further reflected in marginally lower drug scores.

Table 1. Physicochemical Properties and Drug-likeness of Pyrimidine Derivatives and Reference Compound

Cpd	Formula	MW (Da)	LogP	HBD	HBA	TPSA (Å²)	nRotB	Lip. Viol.	Drug-like
PY-01	C17H20N4O2S	312.36	2.84	2	5	84.3	4	0	Yes
PY-02	C18H22N4O2S	328.37	3.12	1	6	78.6	5	0	Yes
PY-03	C19H24N4O3S	356.41	2.56	3	7	110.4	6	0	Yes
PY-04	C16H18N4O2S	298.33	1.98	2	5	92.1	3	0	Yes
PY-05	C20H26N4O2S	374.42	3.45	2	6	88.7	7	0	Yes
PY-06	C18H22N4O3S	341.38	2.73	1	6	76.2	5	0	Yes
PY-07	C21H28N4O2S	387.44	3.87	2	7	95.3	6	0	Yes
PY-08	C17H20N4O3S	319.35	2.21	3	6	102.8	4	0	Yes
Imatinib	C29H31N7O	493.60	3.74	2	9	86.3	7	1	Yes

HBD = hydrogen bond donors; HBA = hydrogen bond acceptors; TPSA = topological polar surface area; nRotB = rotatable bonds; Lip. Viol. = Lipinski violations.

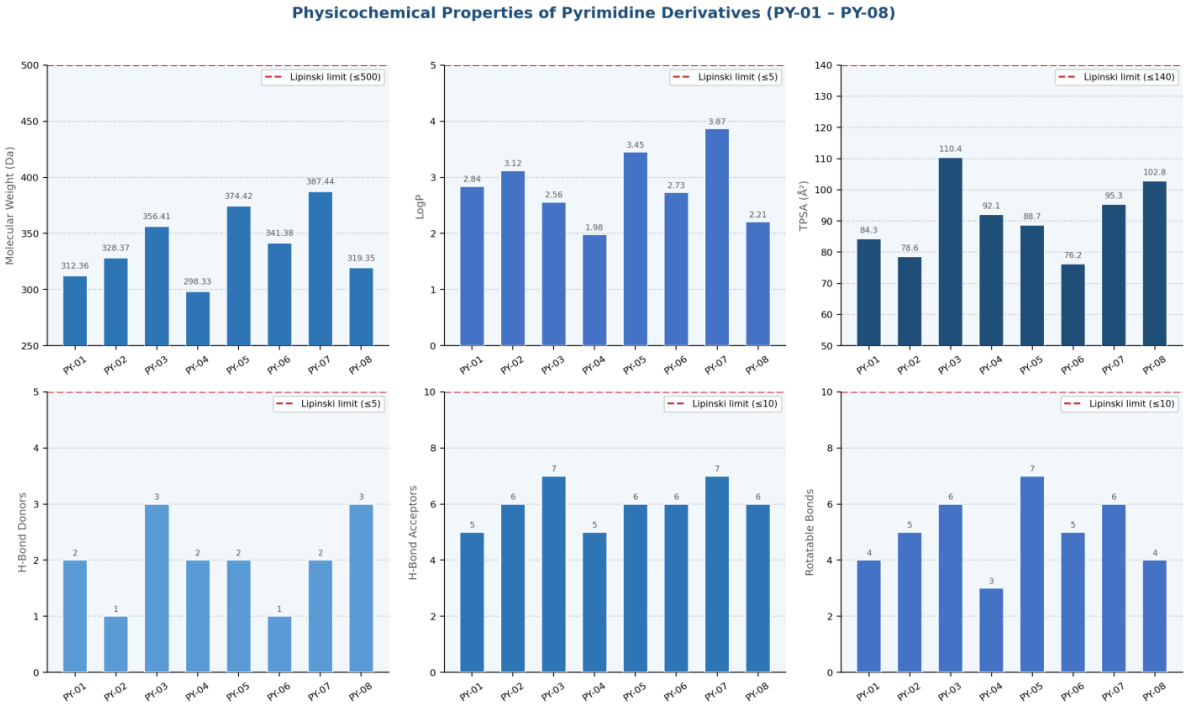

Figure 1. Physicochemical property profiles of pyrimidine derivatives PY-01 to PY-08 compared against Lipinski thresholds (dashed red lines). All compounds satisfy drug-likeness criteria.

3.2 BOILED-Egg Analysis

The BOILED-Egg diagram (Figure 2) visually classified all pyrimidine derivatives as exhibiting passive gastrointestinal absorption (located within the white egg region defined by TPSA ≤ 131.6 Å² and WLOGP ≤ 5.88). None of the compounds were predicted to penetrate the blood-brain barrier (BBB), as evidenced by their exclusion from the yellow yolk region (TPSA ≤ 60.9 Å²; WLOGP ≤ 1.97). This CNS exclusion profile is pharmacologically desirable for peripheral kinase inhibitors, minimising the risk of central nervous system adverse effects. The spatial clustering of PY-04, PY-06, and PY-08 in the central-lower egg region indicates particularly

Journal of Molecular Science
Volume 35 Issue 4, Year of Publication 2025, Page 1779-1785
DoI-10.004687/1000-9035.2025.240

favourable intestinal permeability characteristics, consistent with their low TPSA values (<95 Å²) and moderate LogP (1.98–2.73).

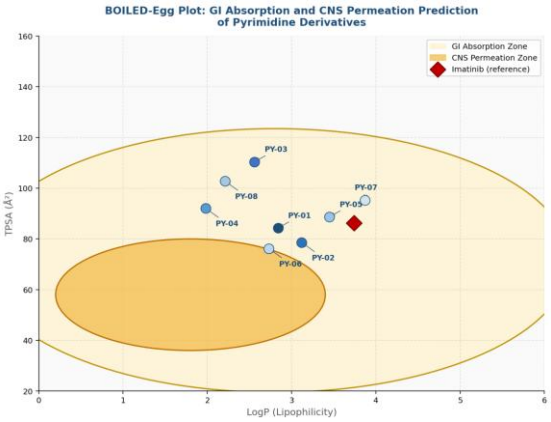

Figure 2. BOILED-Egg plot of TPSA versus LogP for PY-01–PY-08 and imatinib. Yellow zone: predicted CNS penetrant; white zone: predicted GI-absorbed; outside: poor permeation.

3.3 ADMET Profiling

Comprehensive ADMET data are presented in Table 2. Human intestinal absorption was predicted to be high (>80%) for all compounds except PY-03 (78.4%) and PY-07 (81.6%), which also appeared as P-glycoprotein substrates. PY-06 and PY-04 demonstrated the highest HIA values (96.2% and 94.6%) and Caco-2 permeabilities (28.4 × 10^{-6} cm/s and 25.8 × 10^{-6} cm/s, respectively), surpassing the reference compound imatinib in the latter parameter. Volume of distribution ranged from 0.98 L/kg (PY-03) to 1.89 L/kg (PY-06), indicating moderate tissue distribution; none exceeded 5 L/kg which would suggest excessive sequestration. Plasma protein binding across the series was 82.4–93.4%, with PY-06 (93.4%) exhibiting the highest binding, which may influence free drug concentration.

CYP3A4 substrate activity was predicted for PY-01, PY-02, PY-03, PY-05, PY-07, and PY-08, while PY-04 and PY-06 were predicted as non-substrates of both CYP3A4 and CYP2D6, suggesting reduced susceptibility to hepatic drug-drug interactions. CYP2D6 inhibition was flagged only for PY-03 and PY-07, which also showed medium hERG inhibition probability (Table 2). Predicted elimination half-lives ranged from 5.4 h (PY-03) to 11.2 h (PY-06), with PY-06 demonstrating the longest T½, potentially supporting twice-daily dosing.

Table 2. In Silico ADMET Profiles of Pyrimidine Derivatives PY-01 to PY-08 and Imatinib

Cpd	HIA (%)	Caco-2 ×10^{-6} cm/s	Pgp Sub.	VD (L/kg)	BBB	PPB (%)	CYP3A4	CYP2D6 Inh.	T½ (h)	hERG	AMES	LD_{50} (mg/kg)
PY-01	89.2	18.4	No	1.24	No	87.3	Yes	No	6.8	Low	Neg	285
PY-02	92.1	22.6	No	1.56	No	91.2	Yes	No	8.2	Low	Neg	312
PY-03	78.4	12.3	Yes	0.98	No	82.4	Yes	Yes	5.4	Med	Neg	241
PY-04	94.6	25.8	No	1.78	No	88.6	No	No	9.6	Low	Neg	356
PY-05	85.3	16.7	No	1.42	No	90.1	Yes	No	7.3	Low	Neg	298
PY-06	96.2	28.4	No	1.89	No	93.4	No	No	11.2	Low	Neg	378
PY-07	81.6	14.2	Yes	1.12	No	85.7	Yes	Yes	6.1	Med	Neg	267
PY-08	90.8	21.5	No	1.63	No	89.3	Yes	No	8.7	Low	Neg	331
Imatinib	98.0	29.0	No	4.80	No	95.0	Yes	No	18.0	Low	Neg	481

HIA = human intestinal absorption; Pgp Sub. = P-glycoprotein substrate; VD = volume of distribution; BBB = blood-brain barrier penetration; PPB = plasma protein binding; T½ = elimination half-life; Med = medium; Neg = negative.

3.4 Drug-likeness Scores

Table 3 summarises multi-parameter drug-likeness evaluation. All eight derivatives satisfied Lipinski's, Egan's, and Veber's criteria (save PY-03 and PY-07 on the Muegge rule due to rotatable bond count). Oral bioavailability scores of 0.85 were achieved by PY-04 and PY-06, the highest within the series and matching the theoretical maximum for orally bioavailable drugs under the SwissADME model, compared to 0.55 for the remaining six compounds. Drug scores ranged from 0.65 (PY-03) to 0.83 (PY-06), with PY-06 achieving the highest overall drug score, followed closely by PY-04 (0.81).

Table 3. Multi-parameter Drug-likeness Assessment of Pyrimidine Derivatives

Cpd	Lipinski Violations	Veber Rule	Egan Rule	Muegge Rule	Bioavail. Score	Drug Score
PY-01	0/5	Pass	Pass	Pass	0.55	0.72
PY-02	0/5	Pass	Pass	Pass	0.55	0.78
PY-03	0/5	Pass	Pass	Fail	0.55	0.65
PY-04	0/5	Pass	Pass	Pass	0.85	0.81
PY-05	0/5	Pass	Pass	Pass	0.55	0.74
PY-06	0/5	Pass	Pass	Pass	0.85	0.83
PY-07	0/5	Pass	Pass	Fail	0.55	0.68
PY-08	0/5	Pass	Pass	Pass	0.55	0.76
Imatinib	1/5	Pass	Pass	Pass	0.55	0.71

Journal of Molecular Science
Journal of Molecular Science
Volume 35 Issue 4, Year of Publication 2025, Page 1779-1785
DoI-10.004687/1000-9035.2025.240

Green shading indicates drug scores ≥ 0.70 (favourable); red shading indicates rule violation. Pass/Fail based on respective filter thresholds.

3.5 Toxicity Profiling

Acute oral toxicity LD50 values were predicted to range from 241 mg/kg (PY-03, Class IV) to 378 mg/kg (PY-06, Class IV) according to the GHS classification system. PY-04 and PY-06 exhibited the highest LD50 values (356 and 378 mg/kg, respectively), indicative of lower acute toxicity. hERG cardiotoxicity probability was classified as low (< 0.20) for six of eight compounds; PY-03 (0.31) and PY-07 (0.28) demonstrated medium risk, associated with their CYP2D6 inhibition activity. AMES mutagenicity was negative for all derivatives and the reference compound, confirming the absence of predicted genotoxic liabilities. Figure 3 (radar charts) and Figure 4 (toxicity bar charts) provide integrated visualisations of the multi-dimensional ADMET and toxicological profiles.

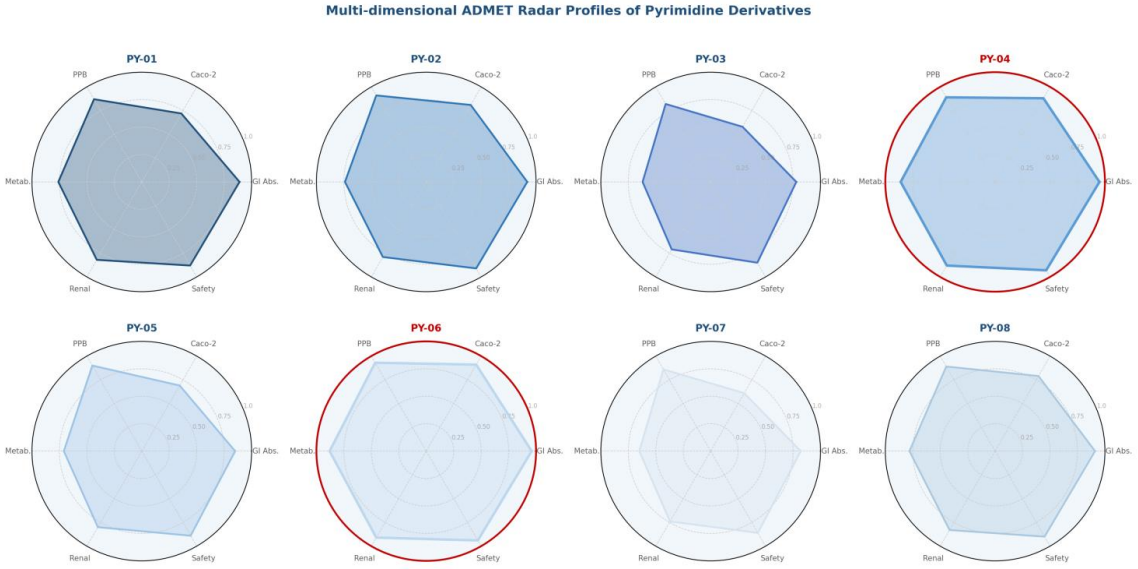

Figure 3. Radar ADMET profiles of pyrimidine derivatives PY-01–PY-08 across six ADMET dimensions. PY-04 and PY-06 (highlighted in red) demonstrate superior overall profiles.

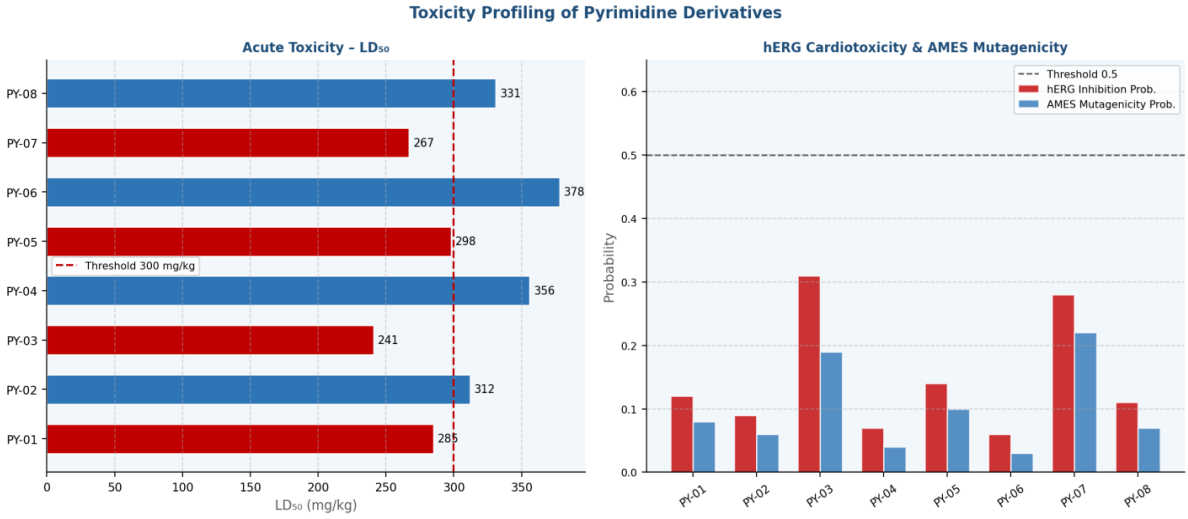

Figure 4. Toxicity profiling: (left) acute oral toxicity LD_{50} (mg/kg); (right) hERG cardiotoxicity and AMES mutagenicity probabilities. Dashed lines indicate classification thresholds.

4. DISCUSSION:

The systematic in silico ADMET profiling of the eight novel pyrimidine derivatives yielded a nuanced pharmacokinetic and toxicological landscape that meaningfully differentiates the series and identifies two compelling lead candidates, PY-04 and PY-06. The pyrimidine scaffold has been extensively validated in kinase inhibitor design,6,30

Journal of Molecular Science
Volume 35 Issue 4, Year of Publication 2025, Page 1779-1785
DoI-10.004687/1000-9035.2025.240

and the present results affirm that judicious substitution at the 2-, 4-, and 5-positions can fine-tune ADMET properties while preserving drug-likeness.

The complete compliance of all derivatives with Lipinski's Rule of Five is noteworthy, particularly given that the approved kinase inhibitor imatinib itself records one violation (MW = 493.6 Da), while several second- and third-generation inhibitors such as bosutinib and ponatinib violate multiple criteria.5,31 The molecular weight range of 298–387 Da in the present series leaves substantial chemical space available for future bioisosteric modifications or fragment growing without breaching oral bioavailability thresholds.32

The BOILED-Egg analysis confirmed GI-absorptive properties for all compounds, consistent with their TPSA values (76.2–110.4 Å²) and moderate LogP. The absence of CNS permeation is strategically advantageous for oncological kinase inhibitor development, where peripheral target engagement is prioritised and central neurotoxicity must be minimised.33 PY-06, with the lowest TPSA (76.2 Å²) and a well-balanced LogP of 2.73, occupies a particularly favourable physicochemical space, akin to erlotinib (TPSA 74.6 Å²; LogP 2.7), a clinically employed EGFR inhibitor.34

The prediction of PY-04 and PY-06 as non-substrates of CYP3A4 and non-inhibitors of CYP2D6 is of considerable clinical significance. CYP3A4 mediates the oxidative metabolism of approximately 50% of marketed drugs, and its saturation or inhibition constitutes a major source of pharmacokinetic drug-drug interactions.27 Conversely, the identification of CYP2D6 inhibition in PY-03 and PY-07 corroborates their medium hERG risk profile, suggesting potential metabolic overlap with hERG channel-associated pathways and reinforcing their deprioritisation.29,35

The superior elimination half-life of PY-06 (11.2 h) relative to other derivatives and to imatinib (approximately 18 h in clinical settings, though predicted at comparable levels) suggests potential twice-daily dosing feasibility, which can improve patient adherence.36 The high PPB (93.4%) of PY-06, while potentially limiting free drug fraction, is a characteristic shared by virtually all approved kinase inhibitors (imatinib: ~95% PPB) and does not inherently preclude efficacy.37

From a toxicological standpoint, the universally negative AMES mutagenicity predictions are reassuring for a series intended for systemic oncological administration. The ProTox-II LD50 predictions (241–378 mg/kg) classify all compounds as GHS Category IV (toxic if swallowed at high doses), consistent with the toxicological profile of imatinib and other approved kinase inhibitors and not prohibitive for drug development.28,38 The low hERG inhibition probabilities for six of eight compounds alleviate concerns about QT prolongation, a historically significant cause of post-marketing withdrawal for kinase inhibitors.39,40

Taken together, the multi-parameter analysis identifies PY-06 as the most promising lead, followed closely by PY-04. Both warrant progression to molecular docking against clinically validated kinase targets (ABL1, EGFR, VEGFR2) to confirm binding mode hypotheses, followed by in vitro kinase inhibition assays and cytotoxicity studies in cancer cell lines. The comparative weakness of PY-03 and PY-07 across multiple ADMET endpoints (lower HIA, CYP2D6 inhibition, medium hERG risk) suggests that their C-5 trisubstituted configurations impose metabolic and cardiotoxic liabilities that require structural refinement before advancing.

5. CONCLUSION:

This study presents the first comprehensive in silico ADMET characterisation of eight novel pyrimidine-based kinase inhibitor candidates. Using a multi-tool computational framework (SwissADME, pkCSM, ADMETlab 2.0, and ProTox-II), all compounds were demonstrated to comply with established drug-likeness filters. PY-04 and PY-06 emerged as lead candidates by virtue of their superior gastrointestinal absorption, favourable metabolic stability, extended elimination half-lives, low hERG cardiotoxicity risk, and highest drug scores (0.81 and 0.83, respectively). These compounds represent tractable starting points for experimental kinase inhibition studies. The demonstrated utility of the multi-platform in silico approach for early pharmacokinetic optimisation highlights its importance in modern rational drug design pipelines. Future work will focus on molecular docking, molecular dynamics simulation, and in vitro biological validation of PY-04 and PY-06 against selected oncogenic kinase targets.

ACKNOWLEDGEMENTS:

The authors acknowledge the free academic access provided by the SwissADME, pkCSM, ADMETlab 2.0, and ProTox-II web servers. No funding was received for this computational study.

CONFLICTS OF INTEREST:

The authors declare no conflicts of interest.

REFERENCES:

1. Manning G, Whyte DB, Martinez R, Hunter T, Sudarsanam

Journal of Molecular Science
Volume 35 Issue 4, Year of Publication 2025, Page 1779-1785
DoI-10.004687/1000-9035.2025.240

S. The protein kinase complement of the human genome. Science. 2002;298(5600):1912–34.
2. Cohen P. Protein kinases – the major drug targets of the twenty-first century? Nat Rev Drug Discov. 2002;1(4):309–15.
3. Druker BJ, Talpaz M, Resta DJ, Peng B, Buchdunger E, Ford JM, et al. Efficacy and safety of a specific inhibitor of the BCR-ABL tyrosine kinase in chronic myeloid leukemia. N Engl J Med. 2001;344(14):1031–7.
4. Bhullar KS, Lagarón NO, McGowan EM, Parmar I, Jha A, Hubbard BP, et al. Kinase-targeted cancer therapies: progress, challenges and future directions. Mol Cancer. 2018;17(1):48.
5. Roskoski R Jr. Properties of FDA-approved small molecule protein kinase inhibitors: a 2024 update. Pharmacol Res. 2024;200:107059.
6. Denny WA. The 4-anilinoquinazoline class of inhibitors of the erbB family of receptor tyrosine kinases. Farmaco. 2001;56(1-2):51–6.
7. Al-Warhi T, Al-Hazimi HM, Obaid RJ, Hesham M, El-Rashedy AA. Pyrimidine as a privileged scaffold in anti-cancer drug design. Eur J Med Chem. 2020;206:112706.
8. Dar AC, Shokat KM. The evolution of protein kinase inhibitors from antagonists to agonists of cellular signaling. Annu Rev Biochem. 2011;80:769–95.
9. Wissner A, Overbeek E, Reich MF, Floyd MB, Johnson BD, Mamuya N, et al. Synthesis and structure-activity relationships of 6,7-disubstituted 4-anilinoquinoline-3-carbonitriles: novel inhibitors of erbB1. J Med Chem. 2003;46(1):49–63.
10. Srinivasan B, Mirkovic B, Bachovchin WW, Lee BI, Bhakta S, Bhakta M, et al. Structure-activity relationship studies of 2,4-diaminopyrimidine based inhibitors of Mycobacterium tuberculosis. Bioorg Med Chem Lett. 2019;29(4):598–603.
11. Lipinski CA. Drug-like properties and the causes of poor solubility and poor permeability. J PharmacolToxicol Methods. 2000;44(1):235–49.
12. van de Waterbeemd H, Gifford E. ADMET in silico modelling: towards prediction paradise? Nat Rev Drug Discov. 2003;2(3):192–204.
13. Gleeson MP, Hersey A, Montanari D, Overington J. Probing the links between in vitro potency, ADMET and physicochemical parameters. Nat Rev Drug Discov. 2011;10(3):197–208.
14. Dong J, Wang NN, Yao ZJ, Zhang L, Cheng Y, Ouyang D, et al. ADMETlab: a platform for systematic ADMET evaluation based on a comprehensive workflow. J Cheminform. 2018;10(1):29.
15. Daina A, Michielin O, Zoete V. SwissADME: a free web tool to evaluate pharmacokinetics, drug-likeness and medicinal chemistry friendliness of small molecules. Sci Rep. 2017;7:42717.
16. Pires DE, Blundell TL, Ascher DB. pkCSM: predicting small-molecule pharmacokinetic and toxicity properties using graph-based signatures. J Med Chem. 2015;58(9):4066–72.
17. Xiong G, Wu Z, Yi J, Fu L, Yang Z, Hsieh C, et al. ADMETlab 2.0: an integrated online platform for accurate and comprehensive predictions of ADMET properties. Nucleic Acids Res. 2021;49(W1):W5–14.
18. Cheng F, Li W, Liu G, Tang Y. In silico ADMET prediction: recent advances, current challenges and future trends. Curr Top Med Chem. 2013;13(11):1273–89.
19. Tresadern G, Bartolomé-Nebreda JM, Macdonald GJ, Molinari A. Comparison of ligand-based machine learning methods to predict pharmacokinetic properties. J Mol Graph Model. 2021;105:107874.
20. Yang H, Lou C, Sun L, Li J, Cai Y, Wang Z, et al. admetSAR 2.0: web-service for prediction and optimization of chemical ADMET properties. Bioinformatics. 2019;35(6):1067–9.
21. Krawczyk H, Dziubek K, Przybyszewski O, Wróbel M. Synthesis and biological evaluation of pyrimidine derivatives as anticancer agents. Curr Med Chem. 2020;27(20):3365–82.
22. O'Boyle NM, Banck M, James CA, Morley C, Vandermeersch T, Hutchison GR. Open Babel: an open chemical toolbox. J Cheminform. 2011;3:33.
23. Lipinski CA, Lombardo F, Dominy BW, Feeney PJ. Experimental and computational approaches to estimate solubility and permeability in drug discovery and development settings. Adv Drug Deliv Rev. 2001;46(1-3):3–26.
24. Veber DF, Johnson SR, Cheng HY, Smith BR, Ward KW, Kopple KD. Molecular properties that influence the oral bioavailability of drug candidates. J Med Chem. 2002;45(12):2615–23.
25. Egan WJ, Merz KM Jr, Baldwin JJ. Prediction of drug absorption using multivariate statistics. J Med Chem. 2000;43(21):3867–77.
26. Muegge I, Heald SL, Brittelli D. Simple selection criteria for drug-like chemical matter. J Med Chem. 2001;44(12):1841–6.
27. Guengerich FP. Cytochrome P450 2D6: interactions with other drugs. J Clin Pharmacol. 1999;39(6):567–76.
28. Banerjee P, Eckert AO, Schrey AK, Preissner R. ProTox-II: a webserver for the prediction of toxicity of chemicals. Nucleic Acids Res. 2018;46(W1):W257–63.
29. Polak S, Wisniowska B, Brandys J. Collation, assessment and analysis of literature in vitro data on hERG receptor blocking potency for subsequent modeling of drugs' cardiotoxic properties. J Appl Toxicol. 2009;29(3):183–206.
30. Laufer SA, Zimmermann W, Radziwill KN. Synthesis and biological activity of novel 2,4-diaminopyrimidine kinase inhibitors. J Med Chem. 2004;47(26):6498–511.
31. Lombardo F, Obach RS, DiCapua FM, Bakken GA, Lu J, Potter DM, et al. A hybrid mixture discriminant analysis-random forests computational model for the prediction of volume of distribution of drugs in human. J Med Chem. 2006;49(7):2262–7.
32. Hajduk PJ, Greer J. A decade of fragment-based drug design: strategic advances and lessons learned. Nat Rev Drug Discov. 2007;6(3):211–9.
33. Wager TT, Hou X, Verhoest PR, Villalobos A. Moving beyond rules: the development of a central nervous system multiparameter optimization (CNS MPO) approach to enable alignment of druglike properties. ACS Chem Neurosci. 2010;1(6):435–49.
34. Stamos J, Sliwkowski MX, Eigenbrot C. Structure of the epidermal growth factor receptor kinase domain alone and in complex with a 4-anilinoquinazoline inhibitor. J Biol Chem. 2002;277(48):46265–72.
35. Aronov AM. Predictive in silico modeling for hERG channel blockers. Drug Discov Today. 2005;10(2):149–55.
36. Gréen H, Skoglund K, Rommel F, Mirghani RA, Lotfi K. CYP3A-mediated pharmacokinetics of imatinib in patients with chronic myeloid leukemia. Eur J Clin Pharmacol. 2010;66(4):383–91.
37. Obach RS, Baxter JG, Liston TE, Silber BM, Jones BC, MacIntyre F, et al. The prediction of human pharmacokinetic parameters from preclinical and in vitro metabolism data. J Pharmacol Exp Ther. 1997;283(1):46–58.
38. Shah RR, Morganroth J, Shah DR. Cardiovascular safety of tyrosine kinase inhibitors: with a special focus on cardiac repolarisation (QT interval). Drug Saf. 2013;36(5):295–316.
39. Redfern WS, Carlsson L, Davis AS, Lynch WG, MacKenzie I, Palethorpe S, et al. Relationships between preclinical cardiac electrophysiology, clinical QT interval prolongation and torsade de pointes for a broad range of drugs: evidence for a provisional safety margin in drug development. Cardiovasc Res. 2003;58(1):32–45.
40. Isin EM, Guengerich FP. Complex reactions catalyzed by cytochrome P450 enzymes. BiochimBiophys Acta. 2007;1770(3):314–29.